

Small-molecule proteostasis regulators for protein conformational diseases

Barbara Calamini¹, Maria Catarina Silva^{1,2}, Franck Madoux³, Darren M Hutt⁴, Shilpi Khanna⁵, Monica A Chalfant⁴, S Adrian Saldanha³, Peter Hodder³, Bradley D Tait⁵, Dan Garza⁵, William E Balch⁴ & Richard I Morimoto^{1*}

Protein homeostasis (proteostasis) is essential for cellular and organismal health. Stress, aging and the chronic expression of misfolded proteins, however, challenge the proteostasis machinery and the vitality of the cell. Enhanced expression of molecular chaperones, regulated by heat shock transcription factor-1 (HSF-1), has been shown to restore proteostasis in a variety of conformational disease models, suggesting this mechanism as a promising therapeutic approach. We describe the results of a screen comprised of ~900,000 small molecules that identified new classes of small-molecule proteostasis regulators that induce HSF-1-dependent chaperone expression and restore protein folding in multiple conformational disease models. These beneficial effects to proteome stability are mediated by HSF-1, FOXO, Nrf-2 and the chaperone machinery through mechanisms that are distinct from current known small-molecule activators of the heat shock response. We suggest that modulation of the proteostasis network by proteostasis regulators may be a promising therapeutic approach for the treatment of a variety of protein conformational diseases.

Proteostasis regulates the functional properties of the proteome to minimize the damage of misfolded and aggregated proteins through a network of pathways for protein synthesis, folding, trafficking and degradation^{1,2}. Loss of proteostatic control has been implicated in aging and in multiple disorders of protein misfolding, including metabolic diseases, cancer and neurodegenerative diseases^{1–3}. Eukaryotic cells have developed compartment-specific quality-control mechanisms for proteome maintenance, to guide protein folding and transport and to direct faulty proteins for refolding or clearance. Likewise, each compartment induces a cell stress response to detect and restore balance: the heat shock response (HSR) for cytoplasmic folding and misfolding and the unfolded protein responses (UPRs) in the endoplasmic reticulum⁴ and mitochondria⁵. Across these compartments are other stress responses that detect specific classes of protein damage caused by metal stress and antioxidants (antioxidant response element signaling pathway, ARE)^{3,6,7}.

The cytosolic HSR is governed by a family of heat shock factors, of which HSF-1 is essential for proteotoxic stress and the regulation of heat shock proteins (Hsps)⁸. Many Hsps are molecular chaperones that guide the conformation of proteins during biogenesis and prevent the misfolding and aggregation that interfere with cellular function⁹. Induction of the HSR not only prevents protein damage from persisting but also restores the cell to the pre-stress condition. Despite these essential cellular stress pathways, the chronic expression and accumulation of misfolded, oxidized and aggregated proteins, as occurs in aging and disease, leads to cellular dysfunction when the quality-control machineries become compromised^{10,11}. There is increasing evidence that misfolded proteins expressed in diseases of protein conformation are not efficiently counterbalanced by a compensatory induction of cellular stress responses such as the HSR¹¹. Enhancing the activity of HSF-1 and the concentrations

of molecular chaperones by genetic techniques or pharmacological manipulation has been shown to restore proteostasis in several models of disease^{12–20}.

Given the prominent roles of HSF-1 in maintaining cellular proteostasis by upregulation of chaperone expression, there has been substantial effort by researchers in the field to identify new small-molecule proteostasis regulators that modulate HSF-1 activity. Several small-molecule activators of HSF-1 are known^{8,21}, including proteasome inhibitors and compounds that selectively bind to the chaperone Hsp90, including radicicol, geldanamycin and 17-AAG. A plant-derived compound, the triterpenoid celastrol, identified from a consortium screen for molecules with protective effects in models of Huntington's disease and amyotrophic lateral sclerosis (ALS), was shown to potently activate the HSR in mammalian cells. Most recently, a yeast-based high-throughput screen (HTS) identified new small-molecule activators of HSF-1 without any associated proteotoxicity²⁰.

Despite the potential benefits of the small-molecule activators of HSF-1, as shown in multiple cellular and animal models of diseases of protein conformation, further development of these small molecules will be necessary before they can be used as therapeutic agents^{22,23}. For example, although geldanamycin and other derivatives that inhibit Hsp90 are currently in pre-clinical and clinical development for the treatment of a number of different cancers²⁴, their use in diseases associated with protein misfolding may have limited therapeutic potential. Given the imminent challenges facing the care of individuals afflicted with protein conformational diseases and the lack of effective therapeutics for these diseases, we propose that further investigation into small-molecule proteostasis regulators that activate HSF-1 is an urgent need. Here we describe the discovery and characterization of new small-molecule proteostasis regulators that, by enhancing HSF-1 activity,

¹Department of Molecular Biosciences, Rice Institute for Biomedical Research, Northwestern University, Evanston, Illinois, USA. ²Faculty of Sciences, Centre for Biodiversity, Functional and Integrative Genomics (BioFIG), University of Lisboa, Lisboa, Portugal. ³Scripps Research Institute Molecular Screening Center, Lead Identification Division, The Scripps Research Institute, Scripps Florida, Jupiter, Florida, USA. ⁴Department of Cell Biology and Chemical Physiology, Institute for Childhood and Neglected Diseases, The Scripps Research Institute, La Jolla, California, USA. ⁵Proteostasis Therapeutics Inc., Cambridge, Massachusetts, USA. *e-mail: r-morimoto@northwestern.edu

restore proteostasis in multiple diseases of protein conformation. We propose that modulation of the proteostasis network by HSF-1 proteostasis regulators may be a new therapeutic approach for the treatment of both cytosolic and compartment-specific conformation disorders.

RESULTS

Cell-based HTS for small-molecule activators of the HSR

We developed an HTS that measures the activation of the HSR in HeLa cells stably transfected with a heat-shock-inducible reporter containing the proximal human Hsp70.1 promoter sequence upstream of a luciferase (luc) reporter gene (Fig. 1a)^{25,26}. To assess the sensitivity and robustness of the cell-based assay before undertaking the HTS campaigns, we established dose-response profiles using three positive controls: celastrol, cadmium chloride (CdCl₂) and MG132 (Fig. 1b). The derived half-maximal effective concentration (EC₅₀) values for celastrol and MG132 were ~3 μM and 5 μM, respectively, which is in agreement with previous reports²¹. Optimization and miniaturization of the HTS formats were carried out independently at the Scripps Research Institute Molecular Screening Center (SRIMSC) and the Southern Research Institute (SRI) (Supplementary Table 1). MG132, because of its sigmoidal profile, and CdCl₂, because of its ability to strongly induce the reporter (Fig. 1b), were subsequently used as positive controls at the SRIMSC and the SRI, respectively (Supplementary Table 2). Assessment of the key variables in the assay was carried out during the miniaturization and optimization steps to achieve 384- and 1,536-well plate formats (Supplementary Table 1). The Z' values for the miniaturized cell-based assays were all ≥0.6, which is

indicative of consistency and reproducibility across the assays. The HeLa-luc assay was validated by prescreening two different libraries: the 1,280-molecule Library of Pharmacologically Active Compounds from Sigma at the SRIMSC and a 2,000-compound set of known biologically active compounds from MicroSource Discovery Systems at the SRI.

Identification of new small-molecule proteostasis regulators

Two primary screens of 803,587 and 100,000 compounds were performed independently at the SRIMSC and at SRI, respectively. The small-molecule libraries consisted of: (i) 607,408 compounds from the Scripps Drug Discovery library and 196,179 compounds from the Molecular Libraries Probe Production Center Network (MLPCN) library, both run at the SRIMSC; and (ii) 100,000 compounds from the National Institute of Neurological Disorders and Stroke (NINDS) library, run at the SRI. The performance of the assays was consistent across all plates, with robust Z' factors and signal-to-background ratios (Supplementary Fig. 1 and Supplementary Table 2). The data obtained from the primary screens were normalized to each positive control set as 100% activation. The screen performed at the SRIMSC identified 759 primary hits, whereas 37 primary hits were identified by the screen performed at the SRI (Supplementary Table 2).

We excluded false-positive hits by performing a triplicate run on the primary hits that yielded 263 confirmed compounds (Supplementary Table 2). Although the more stringent conditions elicited by CdCl₂ led to a lower number of primary hits, these conditions also identified a smaller fraction of false positives, as shown in the confirmatory secondary assays (Supplementary Table 2). We reordered

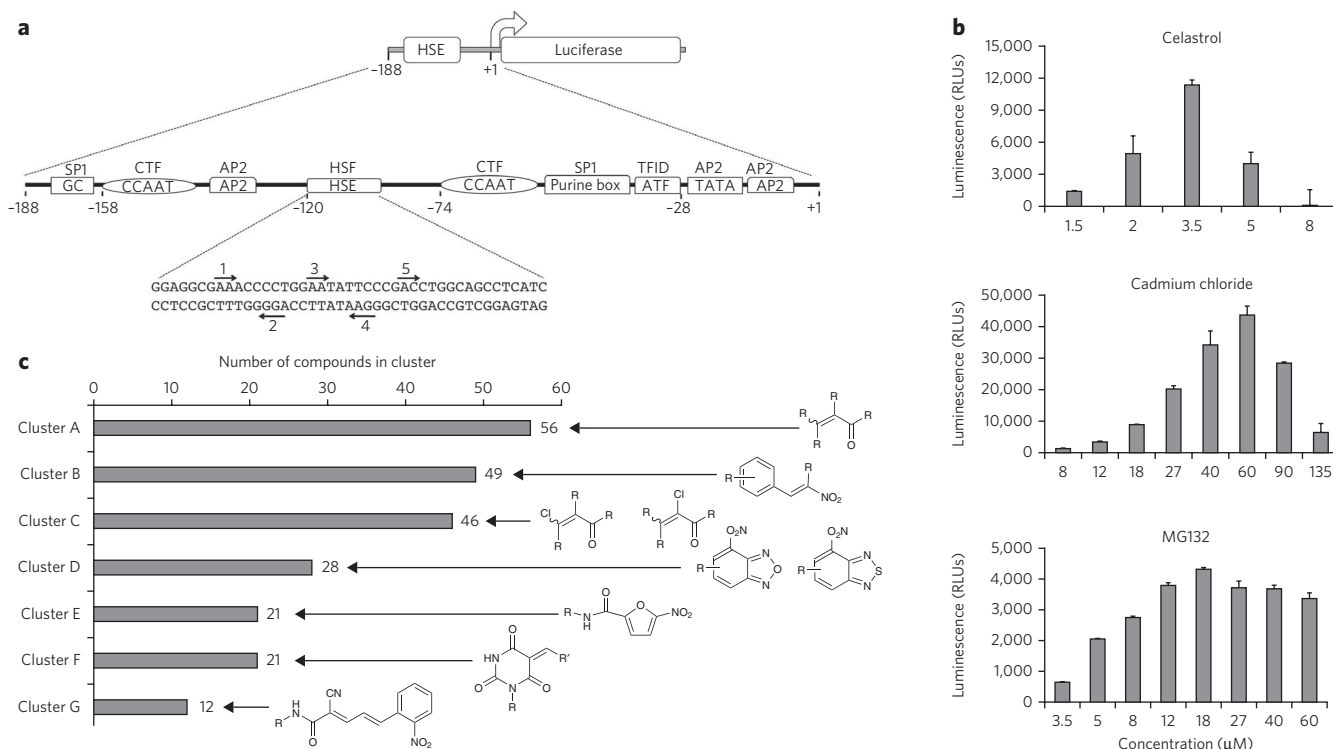
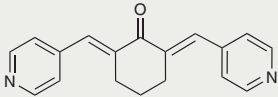
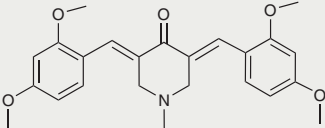
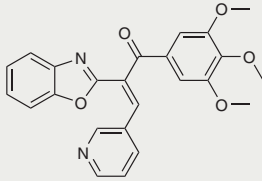
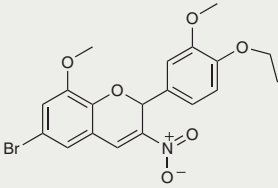
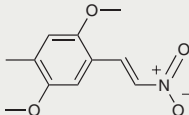
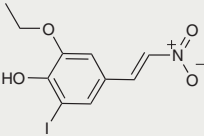
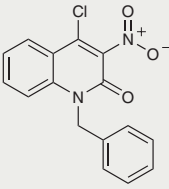
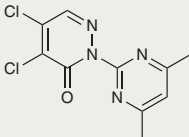
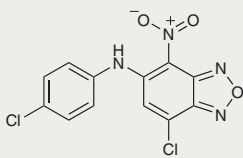
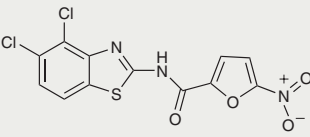
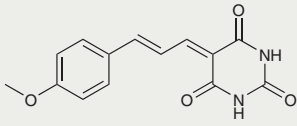
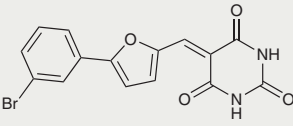
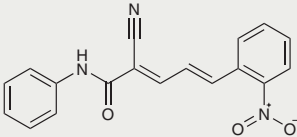
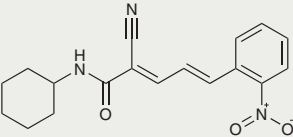


Figure 1 | Identification of small-molecule proteostasis regulators by HTS. (a) HeLa-luc cells were used to screen compound libraries to identify small-molecule proteostasis regulators. The Hsp70.1 promoter (Hsp70.1pr)-luc construct is diagrammed. The sequences of the upstream region of the human Hsp70.1 promoter from +1 to -188 are represented by a line. The locations of transcription factor binding sites are depicted as boxes or circles, and their corresponding genetic elements are indicated. The transcription factors that bind to these regions are indicated above the boxes or circles. The nucleotide sequence of the HSE is shown, and the inverted nGAAn repeats, to which HSF-1 binds, are labeled with arrows and marked as 1-5. (b) HeLa-luc cells were treated with celastrol, cadmium chloride and MG132 at the indicated concentrations, and luciferase activity was measured after 24 h. Each experiment was performed in triplicate. Error bars, s.d. RLU, relative light unit. (c) Confirmed hits ($n = 263$) were clustered according to their chemical substructure, and a total of seven clusters were identified. The number of hits per cluster is shown.

confirmed hit compounds as dry powders from commercial vendors (ChemDiv, Enamine, ChemBridge and Asinex) or resynthesized them for retesting in a full-dose response. We clustered the active compounds by structure with a 0.8 Tanimoto²⁷ cutoff, which we followed with a manual inspection to merge clusters sharing a common

scaffold. This analysis resulted in 233 hits grouped into seven clusters (clusters A through G; **Fig. 1c**) that did not show structural similarities to the remaining 30 hits. Many compounds contained reactive moieties known to activate the HSR, such as reactive α,β -unsaturated carbonyls^{28,29}, but other series had no clear reactive groups.

Table 1 | Chemical structures of the selected small-molecule proteostasis regulators

Cluster A			
	A1	A2	A3
Cluster B			
	B1	B2	B3
Cluster C			
	C1	C2	
Cluster D			
	D1		
Cluster E			
	E1		
Cluster F			
	F1	F2	
Cluster G			
	G1	G2	

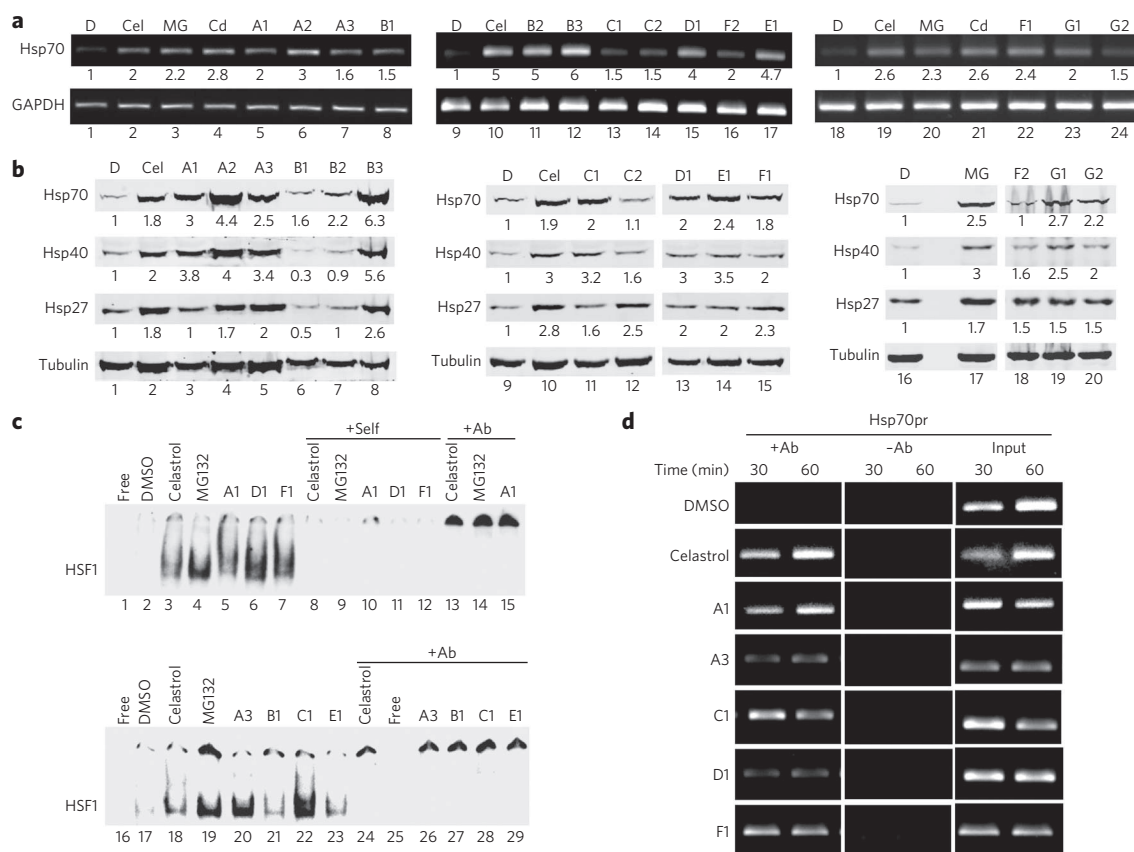


Figure 2 | The small-molecule proteostasis regulators induce Hsp expression by activating HSF-1. (a) HeLa cells were treated with DMSO (D), celastrol (Cel, 3 μ M), MG132 (MG, 10 μ M), CdCl₂ (Cd, 50 μ M) and the indicated proteostasis regulators for 4 h. Similar results were obtained in two independent experiments. Densitometric measurements of Hsp mRNA levels normalized to GAPDH in relation to control DMSO-treated cells were obtained using ImageJ software. (b) Western blot analysis of HeLa cells treated with DMSO, celastrol (3 μ M), MG132 (10 μ M) and the indicated proteostasis regulators. The fold induction was calculated as the ratio of the normalized Hsp value of a compound-treated sample to that of the untreated control. Densitometric measurements of Hsp mRNA levels normalized to tubulin were obtained as in a. (c) A gel mobility shift assay was performed with a [³²P]HSE oligonucleotide and HeLa whole-cell extracts. DMSO, lanes 2 and 17; celastrol (3 μ M), lanes 3 and 18; MG132 (10 μ M), lanes 4 and 19; small-molecule proteostasis regulators (10 μ M), lanes 5–7 and lanes 20–23. Lanes marked +Self (lanes 8–12) contained a 200-fold molar excess of unlabeled complementary oligonucleotide. Lanes marked +Ab (lanes 13–15 and lanes 24–29) contained an HSF-1 antibody. (d) HeLa cells were treated with DMSO, celastrol (3 μ M) and the indicated proteostasis regulators (10 μ M) for 30 min and 60 min, and then chromatin was crosslinked, harvested and immunoprecipitated with HSF-1 antibody (+Ab). The samples were then analyzed using PCR with primers specific for the Hsp70.1 promoter (Hsp70.1pr) and the dihydrofolate reductase promoter. The controls include input DNA and HeLa cells that were not treated with antibodies (–Ab).

The two primary screens performed with different positive controls, chemical libraries and compound concentrations independently identified three common scaffolds (C, E and F; **Fig. 1c** and **Table 1**), providing cross-validation of the cell-based screen. We subsequently tested these active compounds in the HeLa-luc cells to establish dose-response curves and compound toxicity. We determined the EC₅₀ and half-maximal cytotoxicity concentration (CC₅₀) values; most of the hits had a sharp activation profile, with only a few compounds showing sigmoidal dose-response curves. We performed subsequent studies with 14 representative compounds (A1, A2, A3, B1, B2, B3, C1, C2, D1, E1, F1, F2, G1 and G2; **Table 1**) belonging to the largest clusters in A–G (**Fig. 1c**). The dose-response activity and toxicity profiles for the selected compounds are shown in **Supplementary Figure 2**. We refer to these compounds as ‘small-molecule proteostasis regulators’.

Induction of Hsps and HSF-1 by proteostasis regulators

We further validated the results of the HTS screen by directly showing that the expression of endogenous Hsp mRNAs and proteins was induced by representative proteostasis regulators. Exposure of HeLa cells to the proteostasis regulators induced Hsp70 mRNA levels among the different compounds from two-fold to five-fold

(**Fig. 2a** and **Supplementary Fig. 3a**). Likewise, a western blot analysis (**Fig. 2b**) showed that the protein concentrations of multiple chaperones (Hsp70, Hsp40 and Hsp27) were induced from two-fold to six-fold, which was similar to the induction seen in the positive controls (**Fig. 2b** and **Supplementary Fig. 3b**).

The elevated expression of multiple genes encoding Hsps by the proteostasis regulators can be most directly explained by induction of the HSR and the activation of HSF-1. To address whether this is the case, we used electrophoretic gel mobility shift assays (EMSA). Of the 14 proteostasis regulators previously tested for chaperone induction (**Fig. 2a,b**), we selected for this study 7 compounds that were representative of each chemical cluster (A1, A3, B1, C1, D1, E1 and F1). Incubation of HeLa cells with the proteostasis regulators strongly induced the HSF-1 DNA-binding activity (**Fig. 2c**). We showed the specificity of HSF-1 induction using competition with excess unlabeled heat shock element (HSE) oligonucleotide and HSF-1 antibody supershift experiments. We further confirmed the results from the EMSA analysis using chromatin immunoprecipitation (ChIP) experiments. We selected the proteostasis regulators that most strongly induced HSF-1 activation in the gel mobility shift assay (A1, A3, C1, D1 and F1; **Fig. 2c**) for the ChIP analysis, and the results from this analysis showed occupancy of

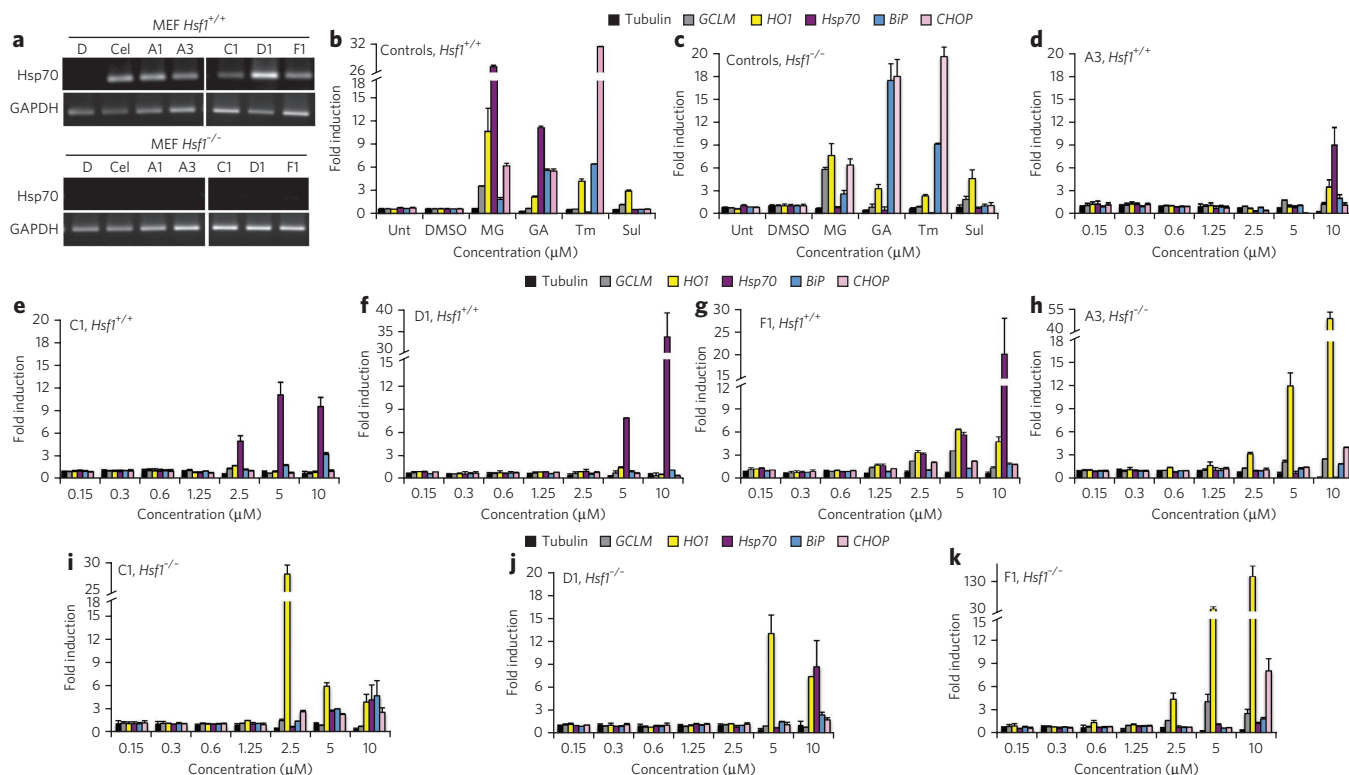


Figure 3 | The proteostasis regulators are HSF-1 dependent. (a) Wild-type (*Hsf1*^{+/+}) and HSF-1 null (*Hsf1*^{-/-}) MEFs were treated for 4 h with DMSO vehicle, celastrol (3 μM) or the indicated proteostasis regulators (10 μM). RNA was extracted and reverse transcribed. PCR reactions were performed on complementary DNA for the indicated transcripts. GAPDH RNA levels were assayed to determine equal loading. (b–k) Wild-type (b,d–g) and *Hsf1*^{-/-} (c,h–k) MEFs were treated for 4 h with either DMSO, MG132 (1 μM), geldanamycin (GA, 1 μM), tunicamycin (Tm, 1 μM), sulforaphane (Sul, 1 μM) or the indicated proteostasis regulators (A3, C1, D1 and F1) at the concentrations shown. Relative expression of multiple cytoprotective genes were measured by real-time quantitative PCR (qRT-PCR), with tubulin serving as the reference.

HSF-1 to the endogenous Hsp70.1 (Fig. 2d and Supplementary Fig. 3c), Hsp40 and Hsp27 promoters (Supplementary Fig. 4) but not to the negative control promoter.

From a chemical mechanism perspective, many previously identified small-molecule inducers of the HSR have been suggested to activate HSF-1 by causing direct protein thiol oxidation. Compounds A1, A3, C1, D1 and F1 contain cysteine-reactive moieties such as unsaturated carbonyls (Supplementary Table 3). No close analogs of these five compounds that lacked these reactive groups were present in the HTS libraries, and, therefore, we did not test them. To determine whether the proteostasis regulators A1, A3, C1, D1 and F1 caused protein thiol oxidation, we tested the effect of the treatment with reducing agents such as N-acetyl cysteine (NAC) or dithiothreitol (DTT). Induction of the HSR by celastrol was inhibited by treatment with either NAC (2 mM) or DTT (250 μM) (Supplementary Fig. 5f,i). Only the activity of the proteostasis regulator F1 was completely inhibited by treatment with NAC and DTT, indicating that F1 may cause oxidative damage by modifying protein cysteine residues (Supplementary Fig. 5e,k). In contrast, the activities of the proteostasis regulators C1 and D1 were only slightly less affected by treatment with NAC and DTT than with F1 (Supplementary Fig. 5c,d,i,j), and activation of the HSR by A1 and A3 was unaffected by this treatment (Supplementary Fig. 5a,b,g,h), indicating that these four proteostasis regulators do not act through protein thiol oxidation.

Proteostasis regulator activity on Hsp genes require HSF-1

Activation of HSF-1 by the proteostasis regulators correlates with the enhanced expression of chaperone genes but does not formally show a requirement for a wild-type HSE sequence or a dependence

on HSF-1. To investigate this, we tested the five proteostasis regulators for their ability to induce luciferase expression in HeLa cells transfected with a mutated HSE sequence fused to a luciferase gene. Cells lacking wild-type HSE did not induce luciferase expression (Supplementary Fig. 6), indicating that an intact HSE is necessary for activation of the HSR by the proteostasis regulators. We then treated wild-type and *Hsf1*^{-/-} mouse embryonic fibroblasts (MEFs) with the proteostasis regulators and showed that induction of Hsp70 mRNA by proteostasis regulators was present in wild-type cells but not *Hsf1*^{-/-} cells (Fig. 3a and Supplementary Fig. 7a). These results provide conclusive evidence that induction of chaperone expression by proteostasis regulators is dependent on the activation of HSF-1.

Proteostasis regulators activate multiple stress pathways

We next examined the gene signature of the proteostasis regulators using a multiplex gene expression analysis to identify additional proteostasis mechanisms regulated by the proteostasis regulators. We asked whether the proteostasis regulators could activate other stress-responsive proteostasis network pathways in addition to the HSR, for example, the UPR and the antioxidant stress response. Therefore, we monitored the expression of the UPR-inducible gene *BiP* (also known as *GRP78* or *HSPA5*), as well as the expression of *HO1* (encoding the antioxidant responsive genes heme oxygenase 1), *GCLM* (encoding the regulatory subunit of glutamate-cysteine ligase) and *GADD153* (also known as *CHOP* or *DDIT3*, the proapoptotic growth-arrest-inducible and DNA-damage-inducible gene 153). We treated wild-type and *Hsf1*^{-/-} MEF cells with proteostasis regulators and the positive controls MG132 and geldanamycin (which induce the HSR, oxidative stress and the UPR), tunicamycin

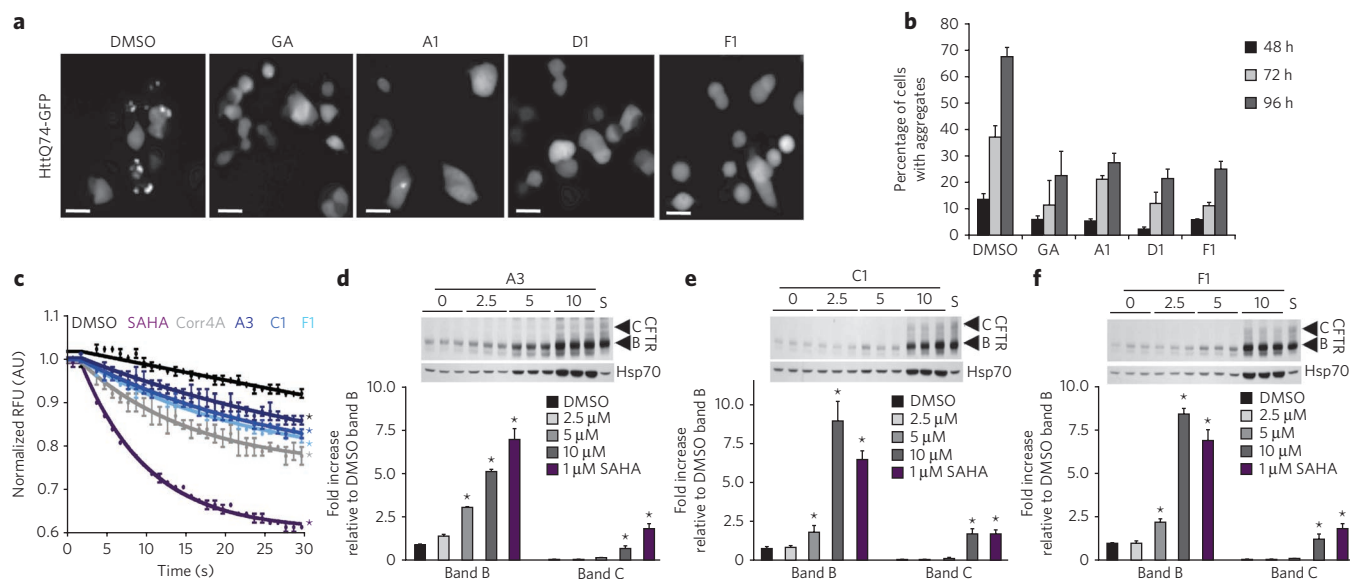


Figure 4 | The proteostasis regulators restore proteostasis in cell-based models of cytoplasmic and compartment-specific conformational diseases.

(a) PC12 cells expressing httQ74-GFP were treated either with DMSO, geldanamycin (200 nM) or with the indicated proteostasis regulators (A1 and F1, 10 μ M or D1, 4 μ M). The representative fluorescence pattern of httQ74-GFP after 72 h of induction is shown. Scale bars, 10 μ m. (b) Quantification of the results shown in a. Cells containing aggregates were counted and are shown as a percentage of the total cells counted. The data shown were derived from three independent experiments. (c) CFBE41o- YFP cells were treated with 0.1% DMSO (black), the positive controls SAHA (5 μ M, purple) and Corrector 4a (Corr4a) (10 μ M, gray) and the proteostasis regulators A3 (10 μ M, dark blue), C1 (10 μ M, royal blue) and F1 (10 μ M, cyan) for 24 h. Fluorescence quenching is indicative of restored Δ F508-CFTR trafficking (data represent the mean \pm s.e.m.; $n = 3$). Color-coded asterisks indicate statistically significant differences ($P < 0.05$, as determined by two-tailed Student's t -test) from the DMSO-treated control at the 30-s time point. (d-f) CFBE41o- cells were treated with 0.1% DMSO, SAHA (5, 1 μ M) and the indicated proteostasis regulators at the concentrations shown in the legend for 24 h. Δ F508-CFTR trafficking was analyzed by monitoring the band B and C glycoforms (data represent the fold increase relative to DMSO band B \pm s.e.m.; $n = 3$) at the various concentrations of proteostasis regulators. The amount of Hsp70 was also monitored by western blot as an indicator of HSF-1 activation. Fifteen micrograms of protein were loaded, and equal loading was confirmed by staining the membrane with Ponceau S. *, statistically significant differences ($P < 0.05$, as determined by two-tailed Student's t -test) from the DMSO-treated control.

(which induces the UPR) and sulforaphane (which activates the antioxidant response) (Fig. 3b,c). Untreated and DMSO-treated cells served as the negative controls (Fig. 3b,c).

We established the proteostasis regulator stress response signatures in wild-type and *Hsf1*^{-/-} MEF cells (Fig. 3d-k). At a range of concentrations of the proteostasis regulators A3, C1, D1 and F1, *Hsp70* mRNA levels were induced from 9- to 30-fold in wild-type MEF cells (Fig. 3d-g). Compound D1 (Fig. 3f) was selective and only induced the expression of *Hsp70*, whereas A3 and C1 strongly upregulated *Hsp70* in addition to inducing a three-fold increase in the expression of *BiP* (A3 and C1) and *HO1* (A3) (Fig. 3d,e). Likewise, compound F1 induced multiple responses; F1 strongly induced *Hsp70* and the oxidative stress response (*HO1* and *GCLM*) genes and, to a lesser extent, the *BiP* gene (2.5-fold) (Fig. 3g).

In performing parallel experiments on *Hsf1*^{-/-} cells (Fig. 3h-k), we noticed that the induction of *HO1* was dramatically enhanced from 12- to 130-fold, whereas the expression of *GCLM* and *BiP* was comparable to that seen in wild-type MEF cells (Fig. 3h-k). These results suggest that upregulation of an antioxidant stress response compensates for HSF-1 deficiency. At the highest concentrations of proteostasis regulators, we observed induction of the cell-death pathway *GADD153* gene. Our previous experiments using DTT treatment indicated that the proteostasis regulators A1, A3, C1 and D1 did not activate the HSR by causing oxidative stress; however, we observed a potent induction of the antioxidant-responsive gene *HO1* in the absence of HSF-1 (Fig. 3h-k). There are at least two possible explanations for this apparent discrepancy. First, if the induction of *HO1* by the proteostasis regulators was a result of the generation of oxidative stress, then we would expect a concerted

upregulation of the antioxidant-responsive *GCLM* gene, as occurs with the compound F1. However, we did not observe this induction in wild-type cells. In addition, transcriptional regulation the *HO1* gene indicates that its expression is regulated by multiple stimuli and is not only dependent on oxidative stress³⁰.

Proteostasis regulators protect against stress and apoptosis

Activation of the HSR and the induction of molecular chaperones have been shown to protect cells from the deleterious consequences of protein damage and apoptosis. Therefore, we tested whether the proteostasis regulators A1, A3, C1, D1 and F1 had cytoprotective properties. Pretreatment with either 42 °C heat shock or the proteostasis regulators A3, D1 and F1 significantly (A3 and D1: P value < 0.01 ; F1: P value < 0.001) protected cells from the cell death induced by a 35-min severe heat shock (45 °C) (Supplementary Fig. 8a). In contrast, the proteostasis regulators A1 and C1 did not have any cytoprotective properties and instead increased the fraction of cell death after the 45 °C treatment compared to the DMSO-treated controls.

We next determined whether the proteostasis regulators protected against the apoptotic cell death induced by oxidative stress. We assessed cellular apoptosis and necrosis after treatment with the proteostasis regulators by staining HeLa cells with annexin V and propidium iodide. In agreement with the cytoprotection data, treatment with the proteostasis regulators A3, D1 and F1 led to a two-fold protection from H₂O₂-induced apoptosis, as indicated by the lower number of annexin V-stained cells compared to untreated cells (Supplementary Fig. 8b). However, cells pretreated with the proteostasis regulators A1 and C1 showed both an apoptotic (A1 and C1) and a necrotic (C1) pattern (Supplementary Fig. 8b).

Proteostasis restoration in models of conformational disease

In addition to its well-established role in maintaining cytoplasmic proteostasis, HSF-1 has also been recently shown to ameliorate endoplasmic reticulum stress³¹. We therefore asked whether the proteostasis regulators, by enhancing chaperone expression, would reduce protein misfolding in diseases in which expression of mutant proteins accumulates in either the cytoplasm or the endoplasmic reticulum.

As a representative cytosolic model, we examined the effects of the proteostasis regulators on huntingtin protein (HTT) aggregation in PC12 cells conditionally expressing human HTT exon 1 containing an expansion of 74 glutamines fused to GFP (referred to here as 'httQ74-GFP')³². In this PC12 cell line, httQ74-GFP aggregates are detected after 48 h of induction. We treated the PC12 cells with the proteostasis regulators and visually monitored them for httQ74-GFP aggregate formation. Incubation with A1, D1 and F1 separately caused an average reduction across experiments from two-fold to three-fold of httQ74-GFP protein aggregates without altering the amounts of httQ74-GFP protein (Fig. 4a,b and Supplementary Fig. 9a–f), whereas the proteostasis regulators A3 and C1 had no effect on httQ74-GFP aggregation, although Hsp70 was induced by A3 and C1 (Fig. 3d,e).

We next investigated the proteostasis regulators in a cellular model of cystic fibrosis. This model corresponds to a human bronchial epithelial cell line (CFBE41o-) stably co-expressing the Δ F508 alteration of the cystic fibrosis transmembrane conductance regulator (Δ F508-CFTR) and a halide-sensing mutant of yellow fluorescent protein (YFP^{H148Q I152L}). Δ F508-CFTR is defective both in trafficking from the endoplasmic reticulum to the plasma membrane and in channel gating³³. Correction of the defective trafficking of Δ F508-CFTR with the proteostasis regulators would lead to an increased amount of active protein at the cell surface, allowing an increased flow of extracellular halides into the cell, which would result in a reduction of YFP fluorescence intensity.

We tested the same proteostasis regulators that we used in the Huntington's disease cell model in cells expressing Δ F508-CFTR, and we obtained results showing that the proteostasis regulators A3, C1 and F1 restored the CFTR-mediated iodide conductance (Fig. 4c and Supplementary Fig. 10a). The extent of YFP quenching that we detected was comparable to that seen with corrector 4a, a commonly used positive control for this assay (Fig. 4c). It is notable that compound F1 is the first characterized small molecule capable of enhancing the correct folding of proteins expressed in two different cellular compartments.

To further confirm that the proteostasis regulators A3, C1 and F1 rescued Δ F508-CFTR trafficking, we monitored the processing of Δ F508-CFTR. Treatment with the proteostasis regulators of CFBE41o- cells expressing Δ F508-CFTR generated higher molecular mass forms of Δ F508-CFTR protein, consistent with full glycosylation (Fig. 4d–f and Supplementary Figs. 10b and 11), indicating that the proteostasis regulators partially rescued the cell-surface expression and maturation of Δ F508-CFTR. In addition, we found that rescue of Δ F508-CFTR trafficking by the proteostasis regulators coincides with Hsp70 upregulation (Supplementary Fig. 11), suggesting that the action of the proteostasis regulators depends on both HSF-1 and the induction of molecular chaperones.

Suppression of aggregation and toxicity in *C. elegans*

We asked whether the efficacy of the proteostasis regulators to reduce httQ74-GFP and Δ F508-CFTR aggregation could also be observed in a *C. elegans* model for the expression of expanded polyglutamines (35 glutamines fused to YFP, referred to as polyQ35-YFP) in body wall muscles, which shows age-dependent aggregation in the muscle cells and organismal toxicity³⁴. This model has many of the characteristics of polyglutamine diseases, such as Huntington's

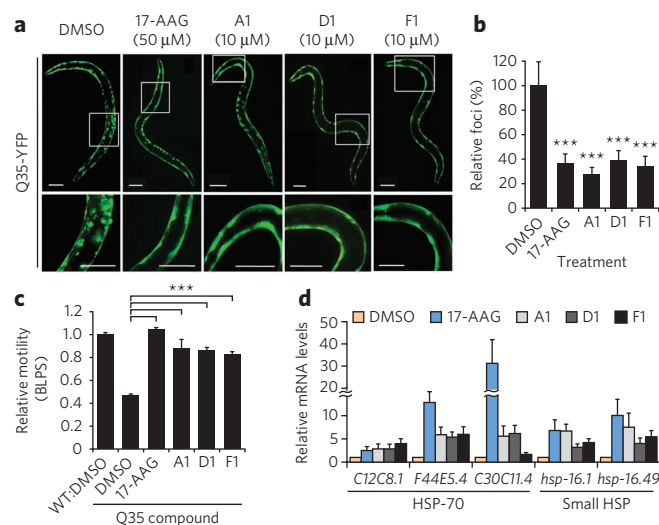


Figure 5 | The proteostasis regulators reduce aggregation and toxicity in *C. elegans* models of diseases associated with polyglutamine expansions.

(a) *C. elegans* expressing YFP-tagged protein containing polyQ35 were treated with either DMSO or the indicated proteostasis regulators at various concentrations (1 μ M, 5 μ M, 10 μ M and 15 μ M) for 4 d; results of treatment with 10 μ M are shown. 17-AAG was used as the positive control (50 μ M). Fluorescence microscopy images show the proteostasis regulators that reduced the aggregation of polyQ35 at a concentration of 10 μ M in 6-day-old animals. In the bottom row are higher magnification images of the boxed areas on the top panels. Scale bars, 0.1 mm. (b) Proteostasis regulators suppress the aggregation of polyQ35, as shown by the quantification of fluorescent foci in 6-day-old animals relative to DMSO control. Error bars, s.e.m. (*** P < 0.001 by t test). (c) Rescue from polyglutamine-associated toxicity was determined by comparing the motility of polyQ35 animals treated with either DMSO alone or the candidate proteostasis regulator compounds (10 μ M) to that of wild-type animals treated with DMSO (wt-DMSO). 17-AAG (50 μ M) was used as the positive control. Error bars, s.e.m. (*** P < 0.001 by t test). BLPS, body length per second. (d) The proteostasis regulators upregulate the mRNA expression of cytosolic chaperones (HSP-70 family members and small Hsps) at the concentrations needed to suppress aggregation and toxicity. Real-time qRT-PCR was performed on samples extracted from animals treated with either DMSO, 17-AAG (50 μ M) or the indicated proteostasis regulators (10 μ M). Error bars, s.d.

disease, and has been a valuable tool in the identification of genetic and chemical modifiers of aggregation and toxicity^{35,36}.

We treated age-synchronized animals expressing polyQ35 with the proteostasis regulators and scored their effects on aggregation and toxicity when the animals were 6 days old. We used 17-AAG as a positive control inducer of the HSR that induces chaperone expression and reduces polyglutamine aggregation^{16,18}. Treatment of *C. elegans* with 17-AAG resulted in a marked reduction in protein aggregates and toxicity (Fig. 5a–c) by inducing the HSR (Fig. 5d). Treatment with the proteostasis regulators A1, D1 and F1 suppressed polyQ35 aggregation (Fig. 5a,b) without affecting overall amounts of polyQ35 protein (Supplementary Fig. 9g,h). Suppression of polyQ35 aggregation also ameliorated aggregation-associated toxicity. Expression of polyQ35 in the body wall muscles reduced the animal's motility by 50% relative to wild-type animals, and treatment of animals expressing polyQ35 with proteostasis regulators restored motility to near that of wild-type animals (80–100% restoration) (Fig. 5c). These results reveal that the proteostasis regulator-induced suppression of polyQ35 aggregation also prevented polyQ35-mediated toxicity.

We then confirmed that the effect of the proteostasis regulators on polyQ35 aggregation and toxicity was associated with expression of molecular chaperones and the induction of the HSR

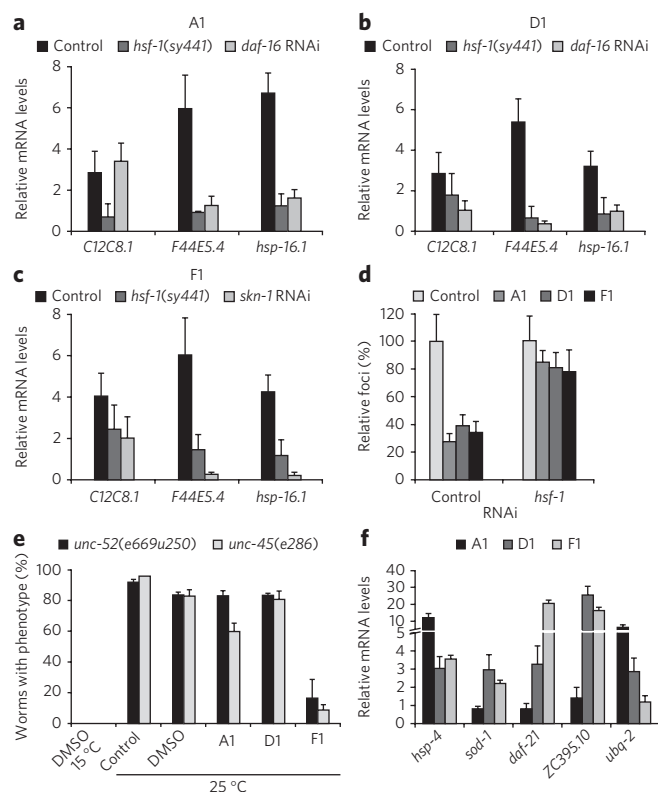


Figure 6 | Chaperone expression and reduction in polyglutamine aggregation in *C. elegans* is HSF-1 dependent. (a–c) For each of the proteostasis regulators, chaperone upregulation is HSF-1 dependent. Wild-type (WT, control) and HSF-1 mutant (*hsf-1(sy441)*) animals were treated with each of the proteostasis regulators or the positive control 17-AAG, and real-time qRT-PCR was performed to show that both HSP-70 (*C12C8.1* and *F44E5.4*) and small-Hsp (*hsp-16.1*) induction does not occur in the *hsf-1* mutant background. For the compounds A1 and D1, DAF-16 also contributed to chaperone upregulation, as SKN-1 did for F1. Error bars, s.d. (d) Suppression of the aggregation of polyQ35 by the proteostasis regulators (shown as a percentage of the total fluorescent foci) was HSF-1 dependent and was not observed when *hsf-1* was downregulated by RNAi. (e) Animals with temperature-sensitive mutations in the muscle proteins UNC-52 (perlecan, causing stiff paralysis) and UNC-45 (myosin assembly, causing an egg-laying defect) were incubated with the indicated proteostasis regulators. At the restrictive temperature of 25 °C, F1 suppressed the muscle dysfunction phenotypes, indicating an improved folding of UNC-52 and UNC-45. (f) Stress-related genes upregulated by each of the proteostasis regulators relative to control (DMSO): *hsp-4* (endoplasmic reticulum HSP-70), *sod-1* (oxidative stress), *daf-21* and *ZC395.10* (HSP-90 and its co-chaperone) and *ubq-2* (ubiquitin). Error bars, s.d.

(Fig. 5d). Chaperone expression was HSF-1 dependent (Fig. 6a–c), and, additionally, downregulation of HSF-1 by RNA interference (RNAi) abrogated the proteostasis regulator-induced protection against the aggregation of polyQ35 (Fig. 6d).

Proteostasis regulators restore metastable protein folding

To examine the basis for induction of the HSR by proteostasis regulators, we asked whether these small molecules caused protein damage and therefore activated a HSR, or, alternatively, whether the proteostasis regulators activated specific homeostasis regulators to induce chaperone expression. To investigate this, we used *C. elegans* strains harboring temperature-sensitive alterations in specific endogenous muscle proteins, including the basement membrane protein perlecan UNC-52 and a myosin-assembly

protein, UNC-45. These conditional alterations do not interfere with protein folding and function at the permissive temperature (15 °C), but they cause a complete loss of protein function at the restrictive temperature (25 °C), resulting in distinctive muscle dysfunction (Fig. 6e, the columns labeled 'DMSO 15 °C' and 'DMSO 25 °C'). These metastable proteins therefore serve as folding sensors that monitor changes in cellular proteostasis¹⁰. To determine whether the proteostasis regulators induce protein misfolding, we incubated both *unc-52(e669su250)* and *unc-45(e286)* animals with the proteostasis regulator A1, D1 or F1 (10 μM) at 15 °C. We reasoned that enhancing the misfolding would unmask the temperature-sensitive phenotypes at the permissive temperature; however, we did not observe this effect. Alternatively, to determine whether the proteostasis regulators enhanced the folding environment, we incubated *C. elegans* with proteostasis regulators, transferred them to 25 °C and scored them for temperature-sensitive phenotypes 2 d later (Fig. 6e). Although the proteostasis regulator A1 caused an intermediate (35%) suppression of the *unc-45(e286)* temperature-sensitive phenotype, we observed the most potent effect with F1, which suppressed both the *unc-52(e669su250)* and *unc-45(e286)* temperature-sensitive phenotypes by 80% and 90%, respectively (Fig. 6e). These results suggest that the proteostasis regulators do not activate the HSR by interfering with cellular protein folding in general, but, rather, they promote the folding of metastable proteins.

Proteostasis regulators require the quality-control machinery

The notable improvement in protein homeostasis after treatment with the proteostasis regulators prompted us to investigate the requirements for other regulatory components of the proteostasis network, such as DAF-16 (a FOXO ortholog, the insulin/IGF-1-mediated signaling transcription factor) and SKN-1 (the oxidative stress response transcription factor). We simultaneously treated polyQ35 animals with the proteostasis regulators and with RNAi to knock down the stress regulators DAF-16 and SKN-1. We examined the effects on induction of *hsp-70* (also known as *C12C8.1* or *F44E5.4*) and the small HSP encoded by *hsp-16.1* and found that A1- and D1-mediated chaperone expression requires both HSF-1 and DAF-16 (Fig. 6a,b), whereas F1 activity is dependent on HSF-1 and SKN-1 (Fig. 6c).

We explored the role of these stress responses on protein folding regulated by the proteostasis regulators by monitoring the gene expression of the downstream targets of SKN-1 and DAF-16 as well as other protein-folding components, including HSP-90, co-chaperone genes, ubiquitin and components of the endoplasmic reticulum HSP-70 protein (UPR). Compounds D1 and F1 elicited the induction of the following genes: *sod-1* (the SKN-1 target), *hsp-4* (UPR in the endoplasmic reticulum) and *hsp-90* and its co-chaperone (*ZC395.1*) (Fig. 6f). A1 induced the *hsp-70* mRNA in the endoplasmic reticulum and the *ubq-2* gene (Fig. 6f and Supplementary Fig. 12). We examined the gene expression of a number of oxidative stress, UPR, mitochondrial UPR and lifespan and aging regulators (Supplementary Fig. 12) and observed that only genes encoding folding and chaperone components were affected by treatment with proteostasis regulators (Fig. 6f). These results indicate that the pathways that are activated to enhance the folding environment depend on HSF-1, DAF-16 and SKN-1 as well as the chaperone and quality-control machinery.

Hsp90 and proteasome are not proteostasis regulator targets

Having shown that the proteostasis regulators themselves do not cause protein misfolding, we examined whether the proteostasis regulators activated the HSR through inhibition of the proteasome or Hsp90 function. For these experiments, we selected the proteostasis regulators A1, A3 and F1 because A1 and F1 suppressed protein aggregation in cellular and *C. elegans* models of conformational diseases and

stabilized folding of temperature-sensitive mutant proteins, and A3 and F1 improved the folding stability of mutant CFTR.

Exposure of HeLa cells to MG132 and lactacystin for 3 h and 6 h (Fig. 7a and Supplementary Fig. 13a) reduced the proteasome activity to 20% relative to DMSO-treated cells (Fig. 7a) leading to increased amounts of polyubiquitinated substrates (Fig. 7b). By comparison, treatment of the HeLa cells with the proteostasis regulators A1, A3 and F1 neither inhibited proteasome activity nor increased the amount of polyubiquitinated proteins (Fig. 7a,b).

We next monitored the effects of the proteostasis regulators on Hsp90 by assessing Hsp90 client protein degradation³⁷. We quantified the amounts of three well characterized Hsp90 client proteins, Cdk4, Raf-1 and Akt, using a western blot analysis of proteostasis regulator-treated HeLa cells. Relative to the DMSO-treated control cells, we observed a reduction in the amounts of the Hsp90 client kinases after 6 h of treatment with the proteostasis regulator A1 (10 μ M) (Supplementary Fig. 13b), whereas treatment with the other two proteostasis regulators (A3 and F1) had no effect. The clearance of these Hsp90 clients was even more notable after 16 h (Supplementary Fig. 13c) and 24 h (Fig. 7c and Supplementary Fig. 7b) of proteostasis regulator treatment, and this effect was comparable to the inhibitory effects of 17-AAG on Hsp90 function.

Because classical Hsp90 inhibitors such as geldanamycin, 17-AAG and radicicol bind competitively to the ATP site of Hsp90, we investigated whether the proteostasis regulators A1, A3 and F1 had a similar mode of action. We therefore tested whether the proteostasis regulators could compete *in vitro* with geldanamycin for binding to the ATP-binding pocket of Hsp90. Whereas the positive control 17-AAG competed effectively with geldanamycin, none of the three proteostasis regulators disrupted the interaction between geldanamycin and Hsp90, even at concentrations in excess of 100-fold relative to the geldanamycin concentration (Supplementary Fig. 13d).

Although the competition assay may suggest that the proteostasis regulator A1 is not an inhibitor of Hsp90 activity, it is also possible that this compound acts through a different mechanism as compared to the known Hsp90 inhibitors. To further confirm that the previous results were not a result of a direct inhibition of Hsp90, we performed a chaperone-dependent protein refolding assay. We monitored the refolding of denatured luciferase in rabbit reticulocyte lysates (RRLs) by measuring the luciferase activity. In the presence of DMSO, luciferase recovered 40–45% of its activity, whereas the presence of 17-AAG (2 μ M) caused only about a 25% recovery in luciferase activity (Fig. 7d). Incubation of RRLs with the proteostasis regulator A1 (10 μ M) did not inhibit luciferase refolding (Fig. 7d). These results indicate that A1 is not a direct inhibitor of Hsp90 activity. Although the proteostasis regulator A1 did not directly inhibit Hsp90 activity, there are possible explanations for the increase in client protein degradation by A1. A1 could disrupt the interaction between Hsp90 and its co-chaperone Cdc37, which is implicated in shuttling kinase clients to Hsp90, or A1 could inhibit Hsp90 activity by binding to a site that is different than the ATP-binding pocket.

DISCUSSION

In this study we describe the results of a large-scale small-molecule screen in human cells for HSF-1-dependent activators of chaperone expression. We identified 263 proteostasis regulators that chemically induce the HSR and result in the activation of HSF-1 and the elevated expression of multiple chaperone gene families. The proteostasis regulators described here are previously unidentified chemical series and, compared to previously identified small-molecule activators of the HSR, do not cause protein misfolding, proteasome inhibition or Hsp90 inhibition. A more in-depth understanding of these proteostasis regulators and their ability to activate the HSR and restore protein folding in multiple disease models offers new

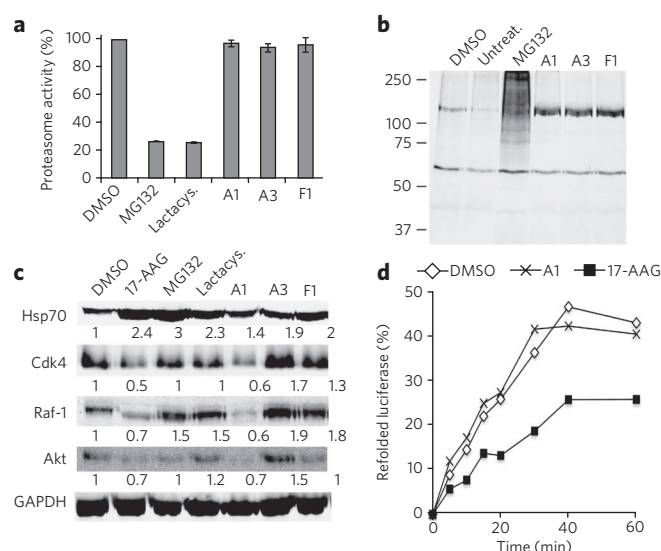


Figure 7 | The proteostasis regulators are not inhibitors of the proteasome or Hsp90. (a) HeLa cells were incubated with either DMSO, MG132 (10 μ M), lactacystin (lactacystin, 6 μ M) or the proteostasis regulator A1, A3 or F1 (10 μ M) for 6 h. Proteasome-associated chymotrypsin activity was assessed using the fluorogenic substrate Suc-Leu-Leu-Val-Tyr-7-amido-4-methylcoumarin. (b) HeLa cells were either left untreated (untreat.) or were treated with DMSO, the proteasome inhibitor MG132 (10 μ M) or the proteostasis regulator A1, A3 or F1 (10 μ M) for 16 h. Whole-cell extracts of HeLa cells were separated by SDS-PAGE, transferred to membranes, stained with Ponceau S to visualize total protein and probed using a rabbit polyclonal antibody to detect ubiquitin. (c) HeLa cells were treated with either DMSO, 17-AAG (2 μ M), MG132 (10 μ M), lactacystin (6 μ M) or the proteostasis regulator A1, A3 or F1 (10 μ M) for 24 h. Concentrations of various Hsp90 client proteins (Cdk-4, Raf-1 and Akt) in equal amounts of whole-cell lysates were assessed using a western blot analysis. GAPDH was used as a loading control. Densitometric measurements of Hsp90 client protein concentrations normalized to GAPDH in relation to control DMSO-treated cells were performed using ImageJ software. (d) Refolding of chemically denatured firefly luciferase was assessed in RRL containing 2 mM ATP in the presence of either DMSO, 17-AAG (2 μ M) or the proteostasis regulator A1 (10 μ M). Luciferase activities are expressed as a percentage of the native enzyme control. The result shown is representative of three experiments.

opportunities and strategies for small-molecule chaperone therapeutics for protein conformational diseases with new specificities and reduced toxicity.

A notable observation is that the proteostasis regulators have complex stress response signatures. In addition to inducing both HSF-1 and the expression of multiple cytoplasmic chaperones, we observed the induction of other major components of the proteostasis network, including the UPR and the antioxidant response genes. Our proteostasis regulator strategy is based on the idea that small molecules can mimic the molecular signals recognized by the cell that are associated with a proteostatic imbalance (Supplementary Scheme 1). This activation of stress-signaling pathways in turn restores the stability and functionality of the proteome. The ability of these proteostasis regulators to activate one or more stress-response pathways suggests a therapeutic approach that uses the cell's biological response to damaged proteins to protect cells against chronic disease. Through this approach, we applied our growing understanding of stress biology to promote the health of the cell. In doing so, we used compounds to enhance the properties of biological pathways that are already employed by the cell to manage proteostasis, even when challenged by stress and disease. We suggest

that this systems and network approach could be an alternative method for drug discovery as we harness the protective abilities of cellular stress responses to protect the cell against the multitude of deficiencies that occur during chronic proteotoxicity and stress.

The central role for HSF-1 in maintaining and restoring proteostasis makes this transcription factor and the HSR attractive targets for therapeutic intervention in conformational diseases. The observation that diverse chemical types have in common the ability to induce the HSR, despite their broad range of activities, supports our proposal that HSF-1 is a stress network hub that integrates multiple stress signaling pathways to coordinate regulatory responses to maintain proteostasis in health, aging and disease. Of the 263 hits identified in this study that activate HSF-1, we focused our attention on the seven major clusters represented by the chemical series: β -aryl- α,β -unsaturated-carbonyls (cluster A), β -nitrostyrenes (cluster B), β -Cl- α,β -unsaturated-carbonyls (cluster C), nitrobenzofurazans (cluster D), nitrofuranylamides (cluster E), unsaturated barbituric acids (cluster F) and 2-cyanopentadienamide (cluster G). These chemical series have a broad range of pharmacological indications and diverse mechanisms of action and, to our knowledge, have not been previously linked to proteostasis and the HSR. For example, compounds in cluster A are chalcone and curcumin analogs and have antibacterial, antioxidant and cancer chemopreventive activities^{38,39}. These compounds are known to inhibit NF- κ B and modulate the Keap1-Nrf2 complex^{40,41}. Nitrobenzofurans (cluster E) have antitubercular activity, and nitrofurans (nitrofurantoin) are currently used as second-line agents for urinary tract infections. The nitroimidazole antibiotics are structurally related; for example, metronidazole is a widely used antibiotic for the treatment of anaerobic bacterial and protozoan infections⁴². Compounds belonging to cluster F are barbiturate analogs associated with anti-inflammatory side effects; in particular, thiobarbiturates reduce the activation of NF- κ B. Thiopental, but not the oxy-analog pentobarbital, is the only barbiturate that has been suggested to activate the HSR, and this property has been attributed to the reactivity of thiopental with protein thiols⁴³. Notably, barbiturate analogs have been previously reported as potentiators of defective Δ F508-CFTR channel gating⁴⁴. Our results reveal unexplored mechanisms by which these chemical classes exert their beneficial effects and suggest new pathways that are involved in the activation of HSF-1. We propose that the ability of barbiturate analogs to rescue defective mutant Δ F508-CFTR channel gating can now be linked to the activation of the HSR, the UPR or both. Likewise, the neuroprotective effects attributed to curcumin⁴⁵, a chalcone analog, may be caused by the induction of chaperone expression⁴⁶. Taken together with the data presented here, we propose that compounds of the same chemical classes identified in our HTS can be reclassified as proteostasis regulators.

We describe a first-generation series of tool compounds that, by activating HSF-1 and other cell-protective stress responses, show efficacy in cellular and animal models of protein conformational diseases. Although we have shown that the proteostasis regulators are effective in multiple misfolding disorders, for example, cystic fibrosis and Huntington's disease, these molecules may have a broader efficacy. For example, proteostasis regulators that restore proteostasis by simultaneously inducing the HSR and the UPR should be able to enhance the folding, trafficking and activity of mutant enzymes in a variety of diseases, including lysosomal storage diseases (Tay-Sachs, Gaucher and Pompe's disease) and retinitis pigmentosa, which require both endoplasmic reticulum and cytoplasmic proteostasis^{47–50}. Likewise, proteostasis regulators selective to the HSR may be beneficial for the treatment of diseases in which the expression of the affected protein is primarily cytoplasmic and nuclear, as in ALS and the multiple forms of spinal cerebellar ataxia. Considering that the pathogenesis of many diseases, such as Alzheimer's disease, Parkinson's disease, ALS and cystic fibrosis

disorders, is also associated with oxidative stress, the activation of the ARE pathway in conjunction with the HSR may be highly beneficial in the treatment of these disorders. In support of this concept, we here show that the small-molecule proteostasis regulator F1, which simultaneously induced both stress-protective pathways, was the only proteostasis regulator that restored proteostasis in distinct cellular compartments.

In conclusion, we propose that the adjustment of the proteostasis network by small-molecule proteostasis regulators of the HSR provides a previously unexploited and potentially powerful approach to obtaining proteome balance in both loss-of-function and gain-of-function diseases by providing a corrective environment based on the principle of proteome balance that is superior to that found in the upregulation of one single pathway. In addition to their usefulness in potential therapeutic development, small-molecule HSR inducers can be used as pharmacological tools for further dissecting the multistep activation pathway of HSF-1. We believe that a better understanding of the regulation of the HSF-1 activation pathway and its signaling mechanisms could lead to the discovery of compounds with stress signatures that are HSF-1 selective or could activate multiple stress pathways that may be effective in the control of diseases of protein conformation.

METHODS

Cell-based high-throughput assays. HeLa-luc cells were used to screen three compound libraries consisting of 903,663 structurally diverse small molecules. A library of 100,000 compounds (NINDS library, http://www.ninds.nih.gov/funding/areas/technology_development/HTS_Facility.htm) was screened at the SRI, and two libraries of 607,408 and 196,179 compounds (Scripps Drug Discovery library and MLPCN library, <http://mli.nih.gov/mli/mlpcn/>) were screened at the SRIMSC. Detailed protocol and analyses are described in the **Supplementary Methods**.

RT-PCR. RNA was purified using the RNeasy Mini kit (QIAGEN) according to the manufacturer's instructions. After the reverse transcription reaction, PCR was performed using PCR primers specific for Hsp70 and GAPDH. The human Hsp70 primers were: 5'-AGAGCCGAGCCGACAGAG-3' (forward) and 5'-CACCTTGCCGTGTGGAA-3' (reverse); the mouse Hsp70 primers were: 5'-CACCAGCAGCTTCCCCA-3' (forward) and 5'-CGCCCTGCGCCTTTAAG-3' (reverse); the human GAPDH primers were: 5'-GTCGGAGTCAACGGATT-3' (forward) and 5'-AAGCTTCCCGTTCTCAG-3' (reverse); and the mouse Gapdh primers were: 5'-TGCACCACCAACTGCTTAG-3' (forward) and 5'-GGATGCAGGGATGATGTTC-3' (reverse). The PCR products were amplified with Taq polymerase (Promega) using standard cycling conditions.

Western blot analysis. An analysis of chaperone expression was carried out using HeLa cells that were treated with selected proteostasis regulators for 8 h. Cells were lysed in a buffer containing 20 mM HEPES (N-2-hydroxyethylpiperazine-N'-2-ethanesulfonic acid; pH 7.9), 25% (vol/vol) glycerol, 0.42 M NaCl, 1.5 mM MgCl₂, 0.2 mM EDTA, 0.5 mM phenylmethylsulfonyl fluoride, 0.5 mM dithiothreitol and 2 mg ml⁻¹ of complete protease inhibitor cocktail (Roche) for 30 min on ice. Fifteen micrograms of whole-cell extracts were run on 7.5% SDS-PAGE gels and transferred to nitrocellulose. Primary antibody incubations were for 12 h at 4 °C in 10% BSA. The following primary antibodies were used: rabbit polyclonal HSF-1 #47 (ref. 25) antibody, mouse monoclonal Hsp70 antibody (4g4, Affinity BioReagents), mouse monoclonal Hsp40 antibody (α Hdj-1 clone 25)²⁵ and mouse monoclonal Hsp27 (MA3-0015, Affinity BioReagents). All primary antibodies were used at a dilution of 1:10,000, except for the Hsp27 antibody, which was diluted 1:500. The β -tubulin antibody (Sigma) was diluted 1:5,000 and used to verify equal protein loading. The secondary antibody was an Alexa Fluor 680 goat mouse IgG antibody diluted 1:5,000 (Invitrogen). The western analysis was performed using the Odyssey system (LI-COR).

EMSA. Detailed protocol is described in the **Supplementary Methods**.

ChIP assays. ChIP was performed essentially as described previously²⁵. Detailed protocol is described in the **Supplementary Methods**.

Effect of NAC and DTT on the proteostasis regulator activity. HeLa-luc cells were seeded in a white 96-well plate at a density of 10,000 cells per well. Cells were pre-treated with either 2 mM NAC or 250 μ M DTT for 1 h before the addition of the positive control celastrol (2.5 μ M or 5 μ M of each) or the selected small-molecule proteostasis regulators (A1, A3, C1, D1 and F1; 2.5 μ M, 5 μ M or 10 μ M of each). Cells were incubated with the compounds for 24 h before acquisition of the luminescence signals. DMSO-treated cells were used as the negative control.

Multiplex gene expression analysis. Wild-type and *Hsf1*^{-/-} MEFs were treated with serially diluted compounds in a seven-point dose-dependent manner. Cell lysates were pooled with mouse eight-gene multiplex probe sets and with eight different sets of magnetic capture beads (Luminex Technology) in a volume of 100 μ l per well. Fold changes in gene expression were obtained for each gene per well by normalizing the raw data first to the DMSO control and then to the TATA-box binding protein housekeeping gene. Detailed protocol is described in the **Supplementary Methods**.

Protein aggregation analysis in PC12 cells. PC12 cells expressing httQ74-GFP were seeded in tissue-culture-treated 96-well plates at 7,500 cells per well and induced with doxycyclin (1 μ g ml⁻¹). Compounds A1, A3, C1, D1 and F1 were used at concentrations ranging from 0.75–25 μ M. Geldanamycin (200 nM) was used as the positive control. The final DMSO concentration was 0.5%. Fluorescence images were taken with a Zeiss Axiovert 200 fluorescence microscope (Carl Zeiss) at $\times 20$ magnification, and images were deconvoluted using Axiovision software. For the quantification of the fluorescence microscopy analysis, approximately 500 cells were counted for each treatment.

Δ F508-CFTR YFP quenching assay. Human bronchial epithelial cells (CFBE41o-) stably expressing Δ F508-CFTR as well as H148Q/I152L-YFP (CFBE41o- YFP) were treated with selected proteostasis regulators in complete growth media and incubated at 37 °C, 5% CO₂ for 24 h. Cells were subsequently stimulated with a final concentration of 10 μ M forskolin and 50 μ M genistein for 15 min before the addition of PBS and NaI (NaCl was replaced with 137 mM NaI). Fluorescence was monitored once a second for a total of 30 s (beginning 3 s before the addition of NaI and ending 27 s after the addition of NaI). Detailed protocol and analyses are described in the **Supplementary Methods**.

Δ F508-CFTR transport assay. CFBE41o- cells stably expressing Δ F508-CFTR were treated with selected compounds (either at 2.5 μ M, 5 μ M or 10 μ M) in complete growth media and maintained at 37 °C, 5% CO₂ for 24 h. Cells were lysed on ice, and the supernatant was collected for analysis. An equal amount of total protein (15 μ g) was separated by SDS-PAGE (8% gel) and transferred to nitrocellulose. The blot was probed overnight at 4 °C for CFTR (3G11 rat monoclonal antibody at 1:500 dilution) and the indicated chaperone proteins. Detailed protocol is described in the **Supplementary Methods**.

C. elegans assays for aggregation and motility defects. The treatment with the chemical compounds was performed in a 96-well plate format in liquid culture. The animals were scored for changes in aggregation (number of fluorescent foci) using the stereomicroscope Leica MZ16 FA microscope equipped for epifluorescence (Leica Microsystems). For the motility assay, the animals' movement was digitally recorded using a Leica M205 FA microscope with a Hamamatsu digital camera C10600-10B (Orca-R2, Leica Microsystems) and Hamamatsu Simple PCI Imaging software. Detailed protocol is described in the **Supplementary Methods**.

Received 23 May 2011; accepted 14 October 2011;
published online 25 December 2011

References

- Balch, W.E., Morimoto, R.I., Dillin, A. & Kelly, J.W. Adapting proteostasis for disease intervention. *Science* **319**, 916–919 (2008).
- Powers, E.T., Morimoto, R.I., Dillin, A., Kelly, J.W. & Balch, W.E. Biological and chemical approaches to diseases of proteostasis deficiency. *Annu. Rev. Biochem.* **78**, 959–991 (2009).
- Morimoto, R.I. Proteotoxic stress and inducible chaperone networks in neurodegenerative disease and aging. *Genes Dev.* **22**, 1427–1438 (2008).
- Ron, D. & Walter, P. Signal integration in the endoplasmic reticulum unfolded protein response. *Nat. Rev. Mol. Cell Biol.* **8**, 519–529 (2007).
- Haynes, C.M. & Ron, D. The mitochondrial UPR - protecting organelle protein homeostasis. *J. Cell Sci.* **123**, 3849–3855 (2010).
- Lichten, P. & Schaffner, W. Putting its fingers on stressful situations: the heavy metal-regulatory transcription factor MTF-1. *Bioessays* **23**, 1010–1017 (2001).
- Vargas, M.R. & Johnson, J.A. The Nrf2-ARE cytoprotective pathway in astrocytes. *Expert Rev. Mol. Med.* **11**, e17 (2009).
- Åkerfelt, M., Morimoto, R.I. & Sistonen, L. Heat shock factors: integrators of cell stress, development and lifespan. *Nat. Rev. Mol. Cell Biol.* **11**, 545–555 (2010).
- Young, J.C., Agashe, V.R., Siegers, K. & Hartl, F.U. Pathways of chaperone-mediated protein folding in the cytosol. *Nat. Rev. Mol. Cell Biol.* **5**, 781–791 (2004).
- Gidalevitz, T., Ben-Zvi, A., Ho, K.H., Brignull, H.R. & Morimoto, R.I. Progressive disruption of cellular protein folding in models of polyglutamine diseases. *Science* **311**, 1471–1474 (2006).
- Gidalevitz, T., Kikis, E.A. & Morimoto, R.I. A cellular perspective on conformational disease: the role of genetic background and proteostasis networks. *Curr. Opin. Struct. Biol.* **20**, 23–32 (2010).
- Sittler, A. *et al.* Geldanamycin activates a heat shock response and inhibits huntingtin aggregation in a cell culture model of Huntington's disease. *Hum. Mol. Genet.* **10**, 1307–1315 (2001).
- Muchowski, P.J. & Wacker, J.L. Modulation of neurodegeneration by molecular chaperones. *Nat. Rev. Neurosci.* **6**, 11–22 (2005).
- Fujimoto, M. *et al.* Active HSF1 significantly suppresses polyglutamine aggregate formation in cellular and mouse models. *J. Biol. Chem.* **280**, 34908–34916 (2005).
- Vacher, C., Garcia-Oroz, L. & Rubinsztein, D.C. Overexpression of yeast hsp104 reduces polyglutamine aggregation and prolongs survival of a transgenic mouse model of Huntington's disease. *Hum. Mol. Genet.* **14**, 3425–3433 (2005).
- Waza, M. *et al.* 17-AAG, an Hsp90 inhibitor, ameliorates polyglutamine-mediated motor neuron degeneration. *Nat. Med.* **11**, 1088–1095 (2005).
- Zhang, Y.Q. & Sarge, K.D. Celastrol inhibits polyglutamine aggregation and toxicity through induction of the heat shock response. *J. Mol. Med.* **85**, 1421–1428 (2007).
- Fujikake, N. *et al.* Heat shock transcription factor 1-activating compounds suppress polyglutamine-induced neurodegeneration through induction of multiple molecular chaperones. *J. Biol. Chem.* **283**, 26188–26197 (2008).
- Hsu, A.L., Murphy, C.T. & Kenyon, C. Regulation of aging and age-related disease by DAF-16 and heat-shock factor. *Science* **300**, 1142–1145 (2003).
- Neef, D.W., Turski, M.L. & Thiele, D.J. Modulation of heat shock transcription factor 1 as a therapeutic target for small molecule intervention in neurodegenerative disease. *PLoS Biol.* **8**, e1000291 (2010).
- Westerheide, S.D. & Morimoto, R.I. Heat shock response modulators as therapeutic tools for diseases of protein conformation. *J. Biol. Chem.* **280**, 33097–33100 (2005).
- Taldone, T., Gozman, A., Maharaj, R. & Chiosis, G. Targeting Hsp90: small-molecule inhibitors and their clinical development. *Curr. Opin. Pharmacol.* **8**, 370–374 (2008).
- Luo, W., Sun, W., Taldone, T., Rodina, A. & Chiosis, G. Heat shock protein 90 in neurodegenerative diseases. *Mol. Neurodegener.* **5**, 24 (2010).
- Solit, D.B. *et al.* Phase II trial of 17-allylamino-17-demethoxygeldanamycin in patients with metastatic melanoma. *Clin. Cancer Res.* **14**, 8302–8307 (2008).
- Westerheide, S.D. *et al.* Celastrols as inducers of the heat shock response and cytoprotection. *J. Biol. Chem.* **279**, 56053–56060 (2004).
- Williams, G.T. & Morimoto, R.I. Maximal stress-induced transcription from the human HSP70 promoter requires interactions with the basal promoter elements independent of rotational alignment. *Mol. Cell. Biol.* **10**, 3125–3136 (1990).
- Butina, D. Unsupervised data base clustering based on Daylight's fingerprint and Tanimoto similarity: a fast and automated way to cluster small and large data sets. *J. Chem. Inf. Comput. Sci.* **39**, 747–750 (1999).
- Amici, C., Sistonen, L., Santoro, M.G. & Morimoto, R.I. Antiproliferative prostaglandins activate heat shock transcription factor. *Proc. Natl. Acad. Sci. USA* **89**, 6227–6231 (1992).
- Trott, A. *et al.* Activation of heat shock and antioxidant responses by the natural product celastrol: transcriptional signatures of a thiol-targeted molecule. *Mol. Biol. Cell* **19**, 1104–1112 (2008).
- Li, C. *et al.* Pharmacologic induction of heme oxygenase-1. *Antioxid. Redox Signal.* **9**, 2227–2239 (2007).
- Liu, Y. & Chang, A. Heat shock response relieves ER stress. *EMBO J.* **27**, 1049–1059 (2008).
- Wytenbach, A. *et al.* Polyglutamine expansions cause decreased CRE-mediated transcription and early gene expression changes prior to cell death in an inducible cell model of Huntington's disease. *Hum. Mol. Genet.* **10**, 1829–1845 (2001).
- Riordan, J.R. CFTR function and prospects for therapy. *Annu. Rev. Biochem.* **77**, 701–726 (2008).
- Morley, J.F., Brignull, H.R., Weyers, J.J. & Morimoto, R.I. The threshold for polyglutamine-expansion protein aggregation and cellular toxicity is dynamic and influenced by aging in *Caenorhabditis elegans*. *Proc. Natl. Acad. Sci. USA* **99**, 10417–10422 (2002).
- Nollen, E.A. *et al.* Genome-wide RNA interference screen identifies previously undescribed regulators of polyglutamine aggregation. *Proc. Natl. Acad. Sci. USA* **101**, 6403–6408 (2004).
- Garcia, S.M., Casanueva, M.O., Silva, M.C., Amaral, M.D. & Morimoto, R.I. Neuronal signaling modulates protein homeostasis in *Caenorhabditis elegans* post-synaptic muscle cells. *Genes Dev.* **21**, 3006–3016 (2007).
- Whitesell, L. & Lindquist, S.L. HSP90 and the chaperoning of cancer. *Nat. Rev. Cancer* **5**, 761–772 (2005).
- Stringer, J.R., Bowman, M.D., Weisblum, B. & Blackwell, H.E. Improved small-molecule macroarray platform for the rapid synthesis and discovery of antibacterial chalcones. *ACS Comb. Sci.* **13**, 175–180 (2011).
- Yadav, V.R., Prasad, S., Sung, B. & Aggarwal, B.B. The role of chalcones in suppression of NF- κ B-mediated inflammation and cancer. *Int. Immunopharmacol.* **11**, 295–309 (2010).
- Dinkova-Kostova, A.T., Massiah, M.A., Bozak, R.E., Hicks, R.J. & Talalay, P. Potency of Michael reaction acceptors as inducers of enzymes that protect

- against carcinogenesis depends on their reactivity with sulfhydryl groups. *Proc. Natl. Acad. Sci. USA* **98**, 3404–3409 (2001).
41. Dinkova-Kostova, A.T. *et al.* Direct evidence that sulfhydryl groups of Keap1 are the sensors regulating induction of phase 2 enzymes that protect against carcinogens and oxidants. *Proc. Natl. Acad. Sci. USA* **99**, 11908–11913 (2002).
 42. Tangallapally, R.P. *et al.* Synthesis and evaluation of nitrofuranylamides as novel antituberculosis agents. *J. Med. Chem.* **47**, 5276–5283 (2004).
 43. Roesslein, M. *et al.* Thiopental protects human T lymphocytes from apoptosis *in vitro* via the expression of heat shock protein 70. *J. Pharmacol. Exp. Ther.* **325**, 217–225 (2008).
 44. Yang, H. *et al.* Nanomolar affinity small molecule correctors of defective Δ F508-CFTR chloride channel gating. *J. Biol. Chem.* **278**, 35079–35085 (2003).
 45. Yang, F. *et al.* Curcumin inhibits formation of amyloid β oligomers and fibrils, binds plaques, and reduces amyloid *in vivo*. *J. Biol. Chem.* **280**, 5892–5901 (2005).
 46. Teiten, M.H., Reuter, S., Schmucker, S., Dicato, M. & Diederich, M. Induction of heat shock response by curcumin in human leukemia cells. *Cancer Lett.* **279**, 145–154 (2009).
 47. Mu, T.W. *et al.* Chemical and biological approaches synergize to ameliorate protein-folding diseases. *Cell* **134**, 769–781 (2008).
 48. Parenti, G. Treating lysosomal storage diseases with pharmacological chaperones: from concept to clinics. *EMBO Mol. Med.* **1**, 268–279 (2009).
 49. Gorbatyuk, M.S. *et al.* Restoration of visual function in P23H rhodopsin transgenic rats by gene delivery of BiP/Grp78. *Proc. Natl. Acad. Sci. USA* **107**, 5961–5966 (2010).
 50. Tam, L.C. *et al.* Prevention of autosomal dominant retinitis pigmentosa by systemic drug therapy targeting heat shock protein 90 (Hsp90). *Hum. Mol. Genet.* **19**, 4421–4436 (2010).
- screening activities; S. Fox, J. West, S. Westerheide, J. Moran, M. Beam and K. Orton for technical assistance; J.S. Pedersen for help developing the worm tracker system; and the Morimoto laboratory, in particular T. Gidalevitz, J. Kirstein, C. Voisine and A. Yu, for helpful comments. PC12 httQ74-GFP cells were provided by D. Rubinsztein (University of Cambridge). Purified Hsp90 β was a gift of A. Chadli (Georgia Health Science University). We thank A. Ciechanover for the rabbit polyclonal ubiquitin antibody (Israel Institute of Technology). The CFBE41o- YFP cells were a gift from L. Galletta (Istituto Giannina Gaslini). This work was supported by the US National Institutes of Health (NIH) Training Grant in Signal Transduction and Cancer T32 CA70085 and the NIH Training Grant in Drug Discovery in Age Related Diseases T32 AG000260 (to B.C.), Portuguese PhD fellowship from the Fundação para a Ciência e Tecnologia (SFRH/BD/28461/2006) (to M.C.S.), NIH grants HL 079442, GM42336 and DK785483 (to W.E.B.), a fellowship from the Canadian Institutes for Health Research (CIHR) (to D.M.H.), the NIH Molecular Library Screening Center Network MH084512 (to F.M., S.A.S. and P.H.) and NIH grants GM038109, GM081192, AG026647 and NS047331 (to R.I.M.).

Author contributions

B.C. and R.I.M. designed the research plan. B.C., M.C.S., F.M., M.A.C., D.M.H., S.K. and S.A.S. designed and performed the research. B.C., M.C.S., F.M., D.M.H., S.A.S., P.H., B.D.T., D.G., W.E.B. and R.I.M. analyzed and interpreted the data. B.C. and R.I.M. wrote the manuscript. All authors reviewed the manuscript.

Competing financial interests

The authors declare competing financial interests: details accompany the full-text HTML version of the paper at <http://www.nature.com/naturechemicalbiology/>.

Additional information

Supplementary information is available online at <http://www.nature.com/naturechemicalbiology/>. Reprints and permissions information is available online at <http://www.nature.com/reprints/index.html>. Correspondence and requests for materials should be addressed to R.I.M.

Acknowledgments

We acknowledge J. Maddy, the SRI and the NINDS for support in performing the primary screen; P. Chase and P. Baillargeon of Scripps Florida for executing the SRIMSC